Supporting Materials for

Global Warming Amplifies Inland Compound Risks from Tropical Cyclones

Dan Fu[1*], Xue Liu[2], Frederic S. Castruccio[3], Gan Zhang[4], Ping Chang[1,2], Gokhan Danabasoglu[3]

Corresponding author: fudan1991@tamu.edu

The PDF file includes:

Supplementary Figures 1-9

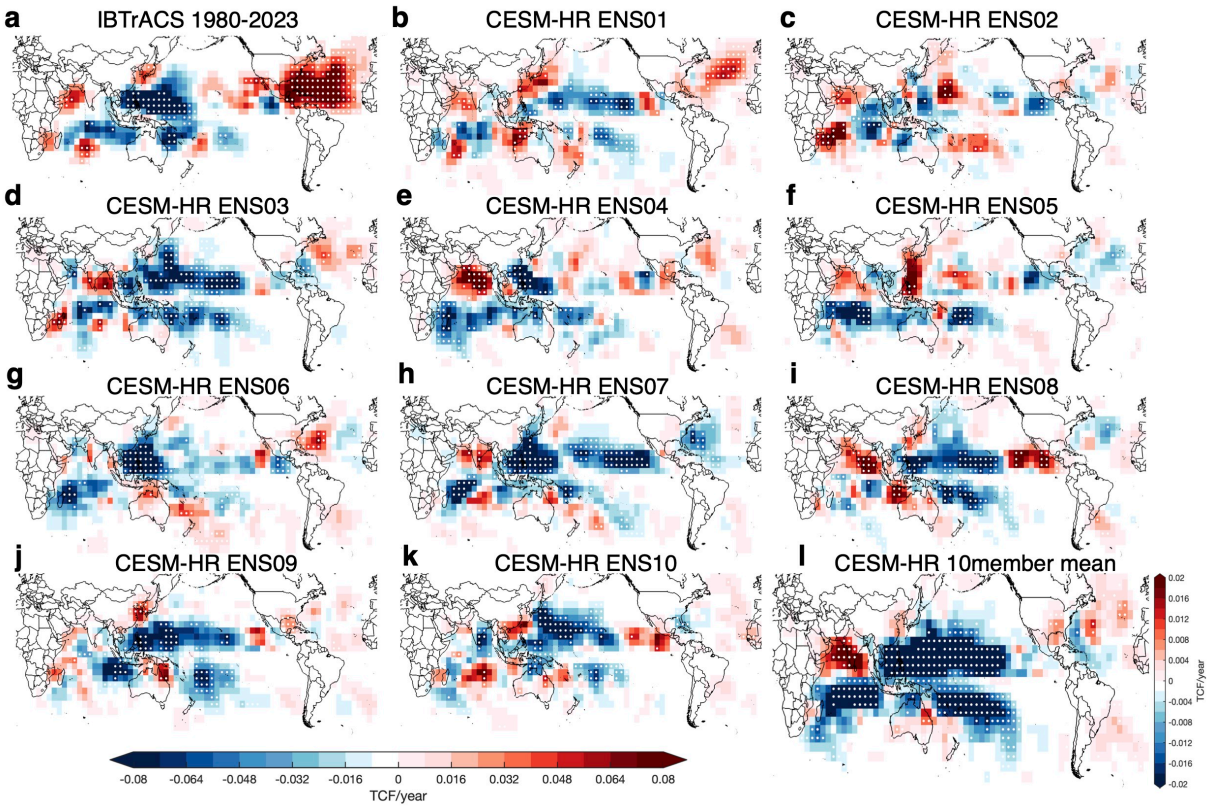

Supplementary Figure 1. (a) Observed and CESM-HR simulated TC track density trend during 1980-2023 (units: TC frequency per year). (b)-(k) Shows each of the 10-member CESM-HR ensemble, and (l) denotes ensemble mean. White dots indicate grid cells where the linear trend is statistically significant at the 90% confidence level (Mann–Kendall test). We note that colormap scale is 4 times smaller in 10-member ensemble mean (l) than observation and individual ensemble member (a-k). Among 10-member ensemble, ensemble #1 closely replicate the observed TC track density trend during 1980-2023.

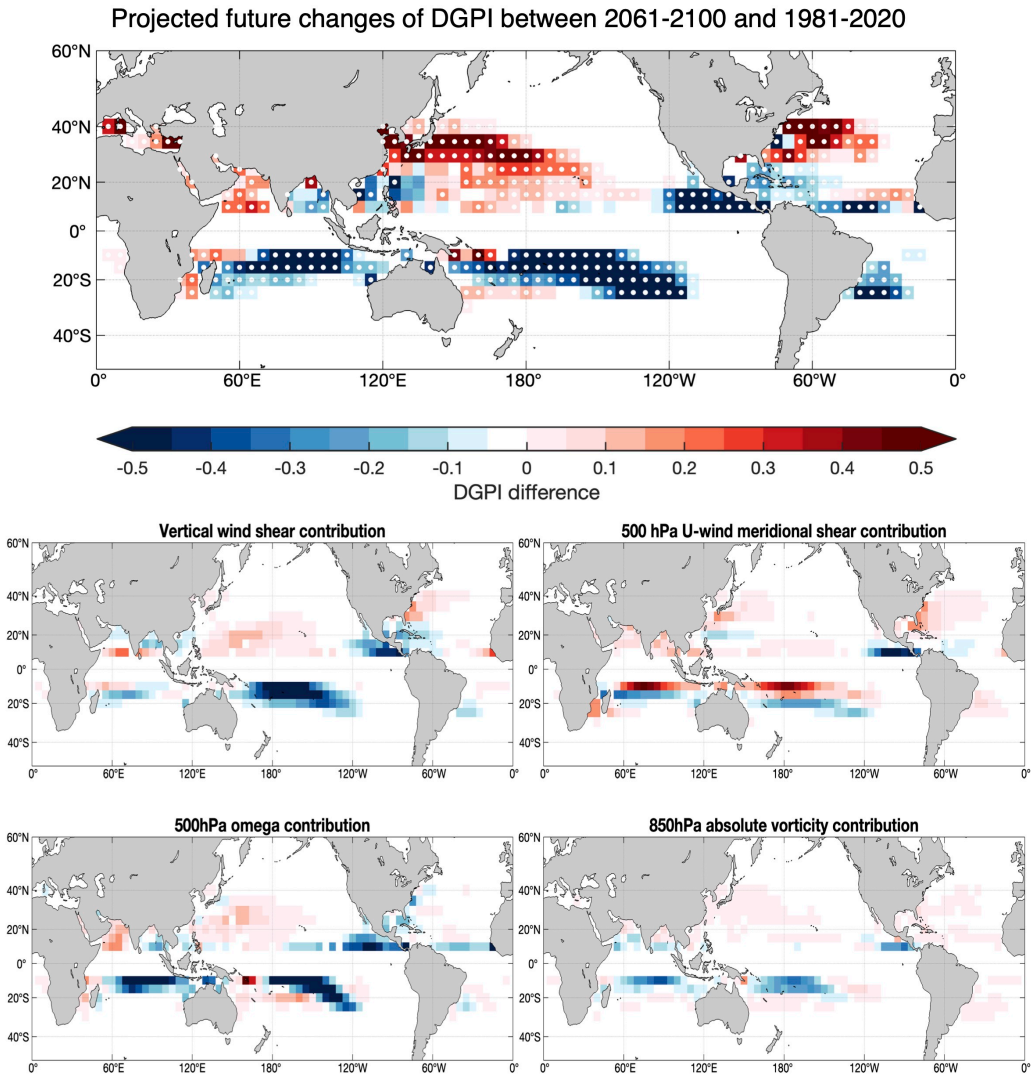

Supplementary Figure 2. Projected future changes in CESM-HR ensemble-averaged TC dynamical genesis potential index (DGPI). The positive (negative) anomalies indicate that the large-scale environmental conditions become more (less) conducive for TC genesis. White dots indicate statistically significant TC track density differences at the 95% confidence level (two-sided t-test). The relative contribution from each factor (850 and 200 hPa vertical wind shear, 500 hPa shear vorticity of zonal wind, 500 hPa vertical motion, and 850 hPa absolute vorticity) to total DGPI changes are shown in the lower panels (see details in Methods).

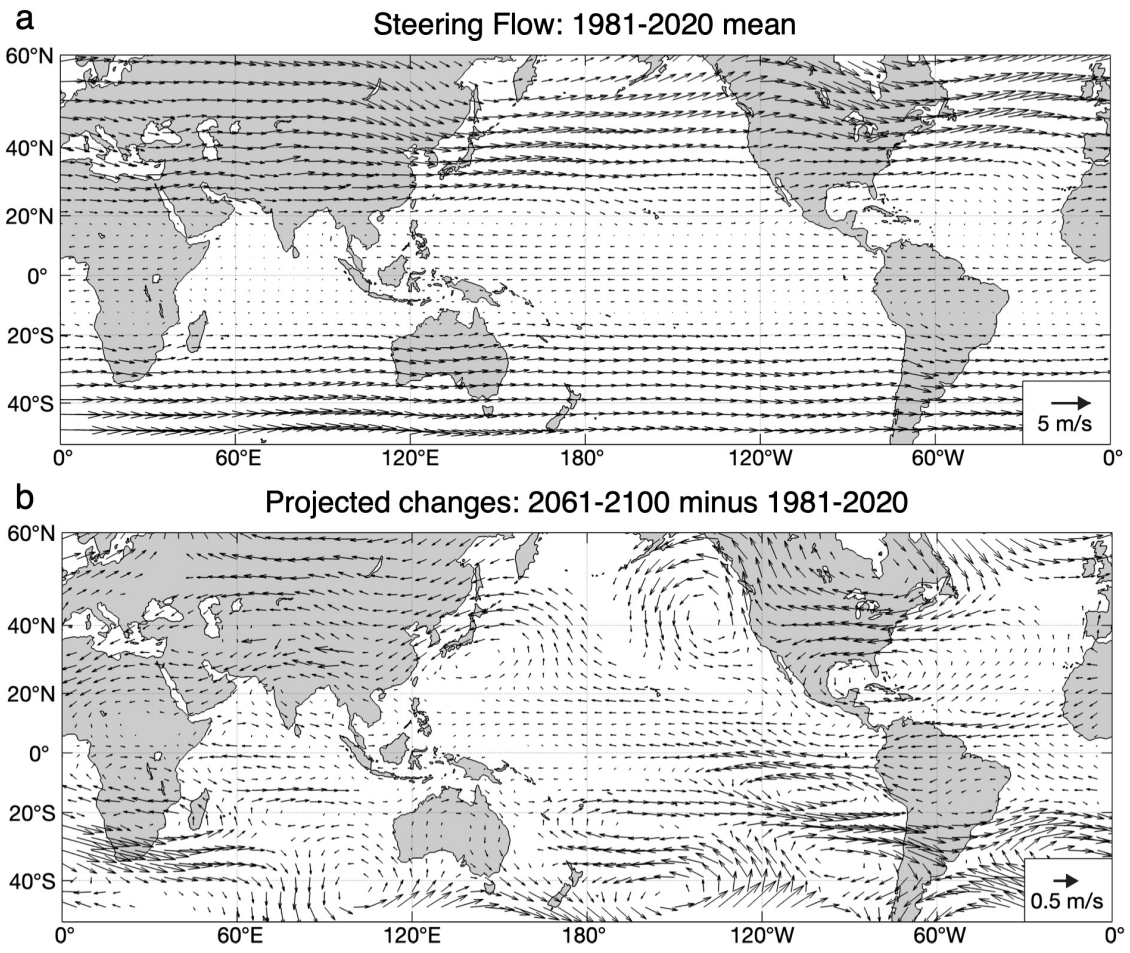

Supplementary Figure 3. CESM-HR ensemble-averaged TC steering flows. TC steering flows are computed using monthly mean 300–800 hPa mass-weighted zonal and meridional wind velocity. (a) Annual average during 1981–2020, and (b) projected future changes between 2061–2100 and 1981–2020. Only the regions that the projected differences are statistically significant at the 95% confidence level (two-sided t-test) are shown.

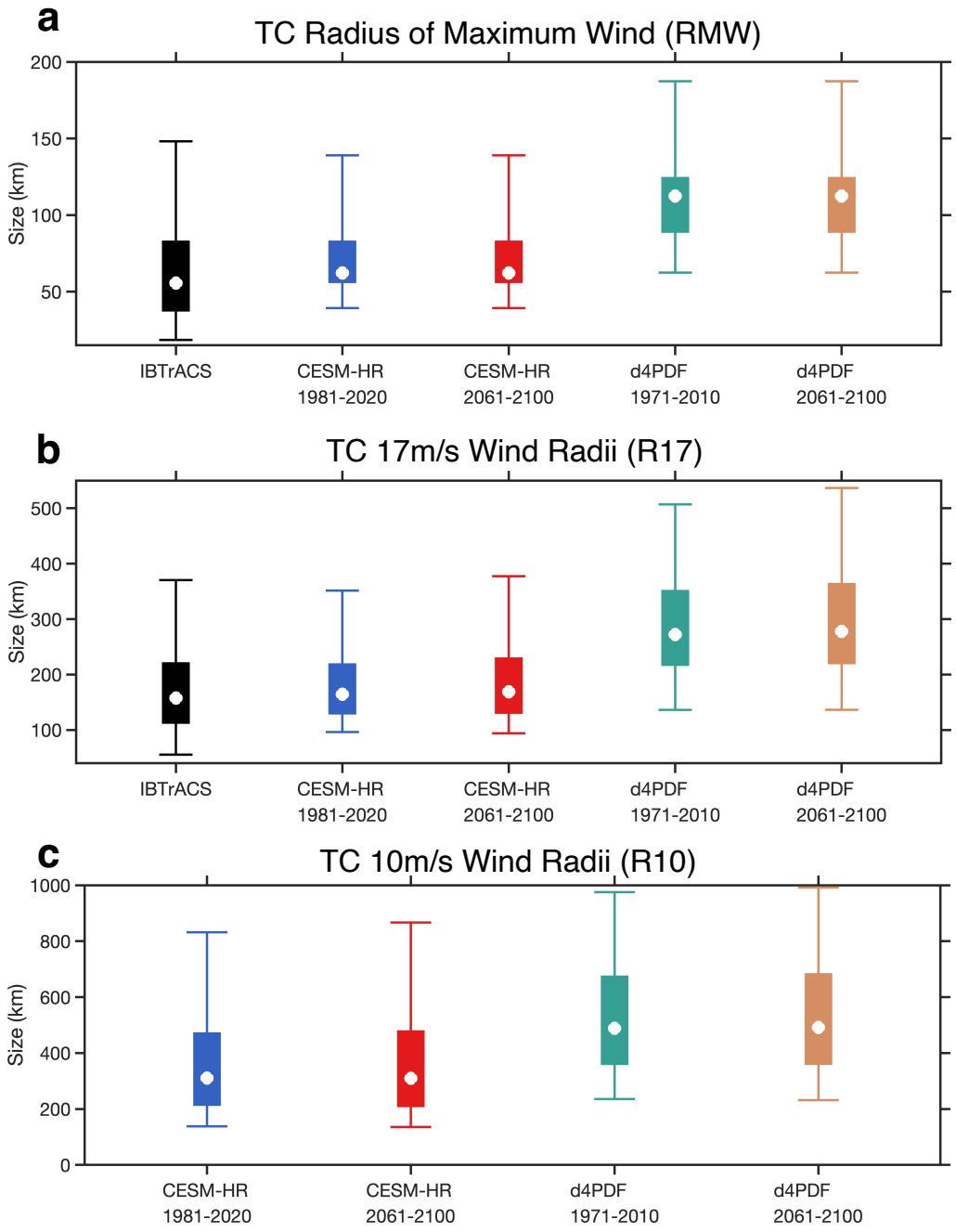

Supplementary Figure 4. Verification of TC sizes in CESM-HR and d4PDF simulation ensembles. (a) TC radius of maximum wind (RMW; units: km) in the IBTrACS (black), CESM-HR historical (blue), future warmer climate (red), d4PDF historical (green), and future warmer climate (brown). The box-whisker plots show the median (white dot), interquartile range (boxes), and 5th to 95th percentile (whiskers). (b) And (c) are similar, but for the 17 m/s (~34 knots) and 10 m/s wind radii (R17 and R10), respectively. Note that, the IBTrACS does not provide R10 information.

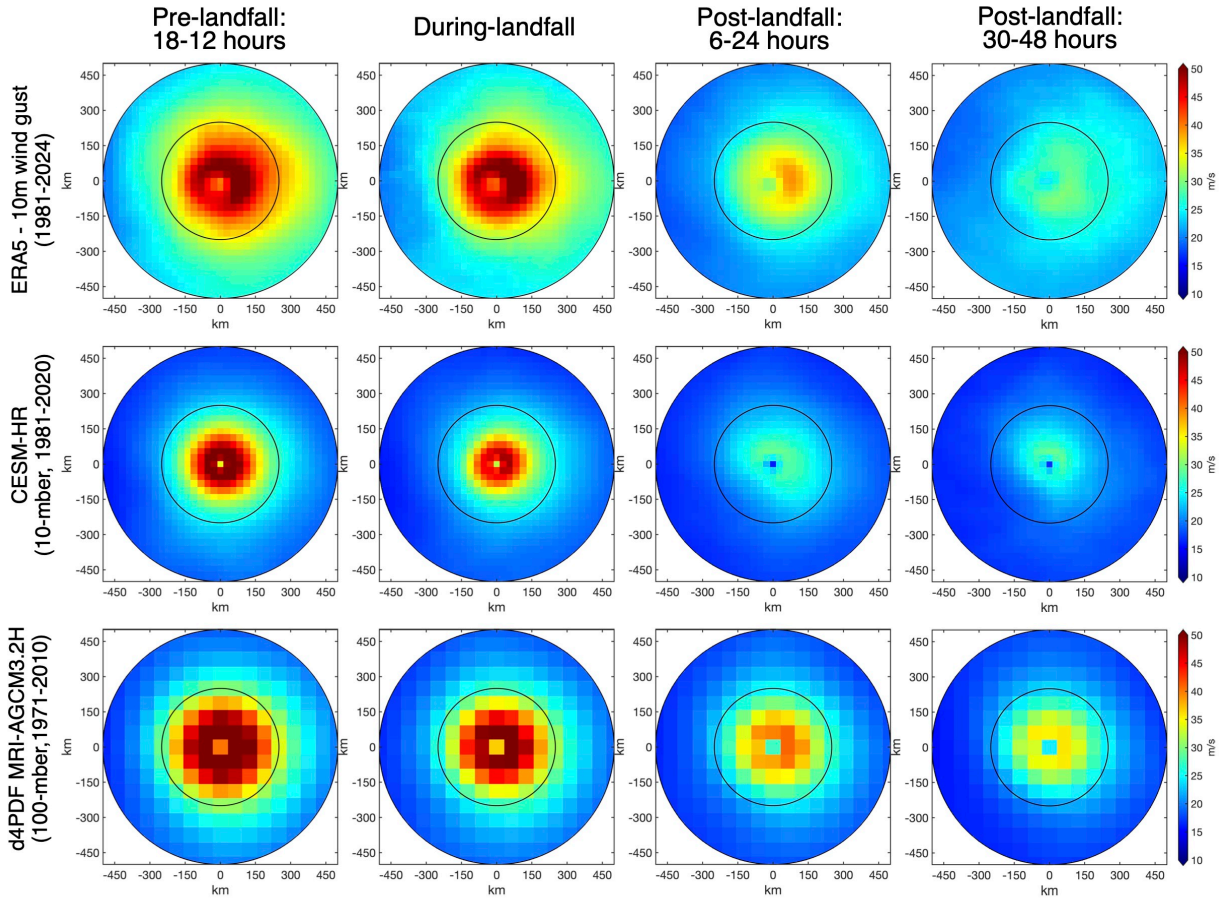

Supplementary Figure 5. Validation of extreme (>99th percentile) TC surface wind speed (units: m/s) in ERA5 (top), CESM-HR (middle), and d4PDF MRI-AGCM3.2H (bottom). Axes indicate distance (km) from the TC center; inner and outer circles denote 200 km and 500 km radii, respectively. The columns (from left to right) show composites of extreme TC surface wind speed occurring 18–12 hours before landfall, during landfall, 6–24 hours after landfall, and 30–48 hours after landfall, respectively.

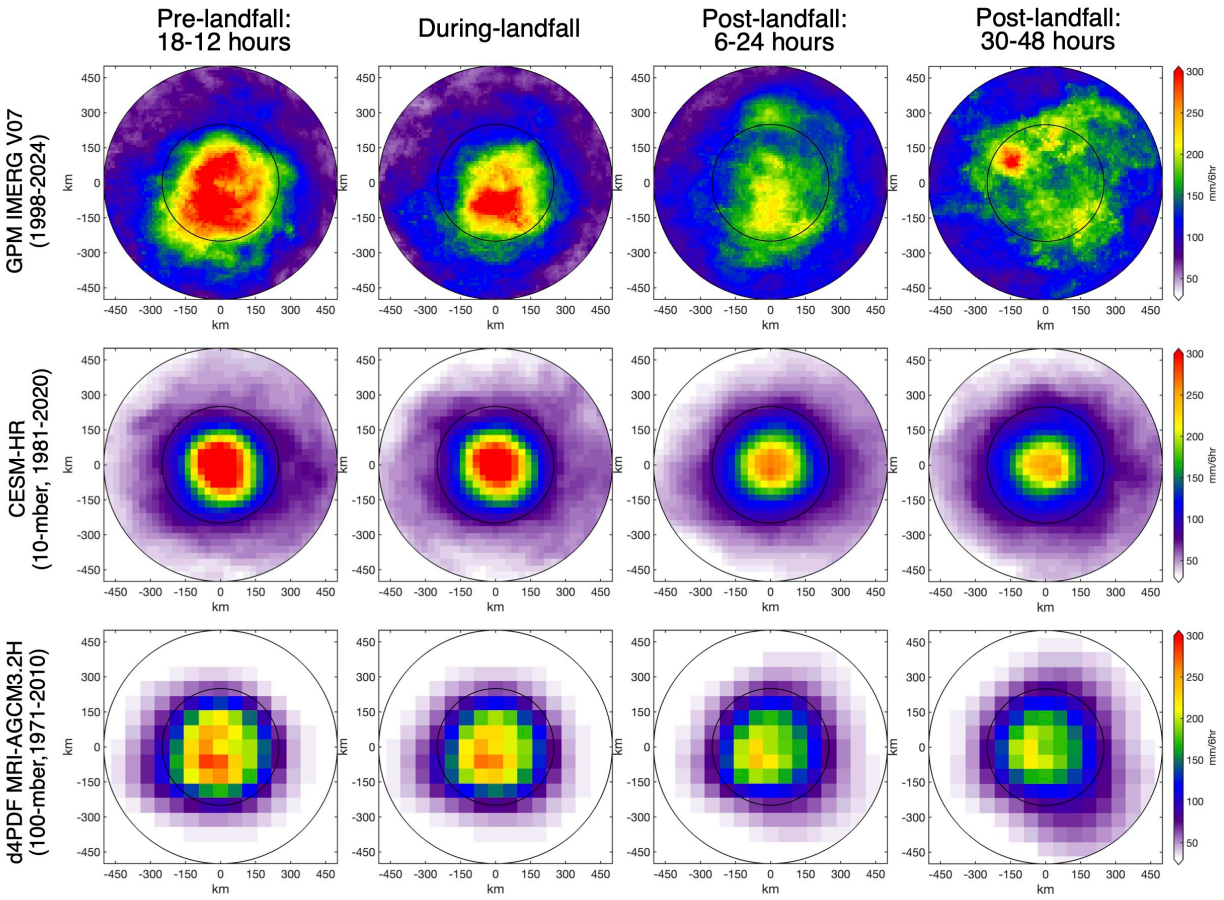

Supplementary Figure 6. Validation of extreme (>99th percentile) TC precipitation rate (units: mm/6 hours) in GPM IMERG V07 (top), CESM-HR (middle), and d4PDF MRI-AGCM3.2H (bottom). Axes indicate distance (km) from the TC center; inner and outer circles denote 200 km and 500 km radii, respectively. The columns (from left to right) show composites of extreme TC surface wind speed occurring 18–12 hours before landfall, during landfall, 6–24 hours after landfall, and 30–48 hours after landfall, respectively.

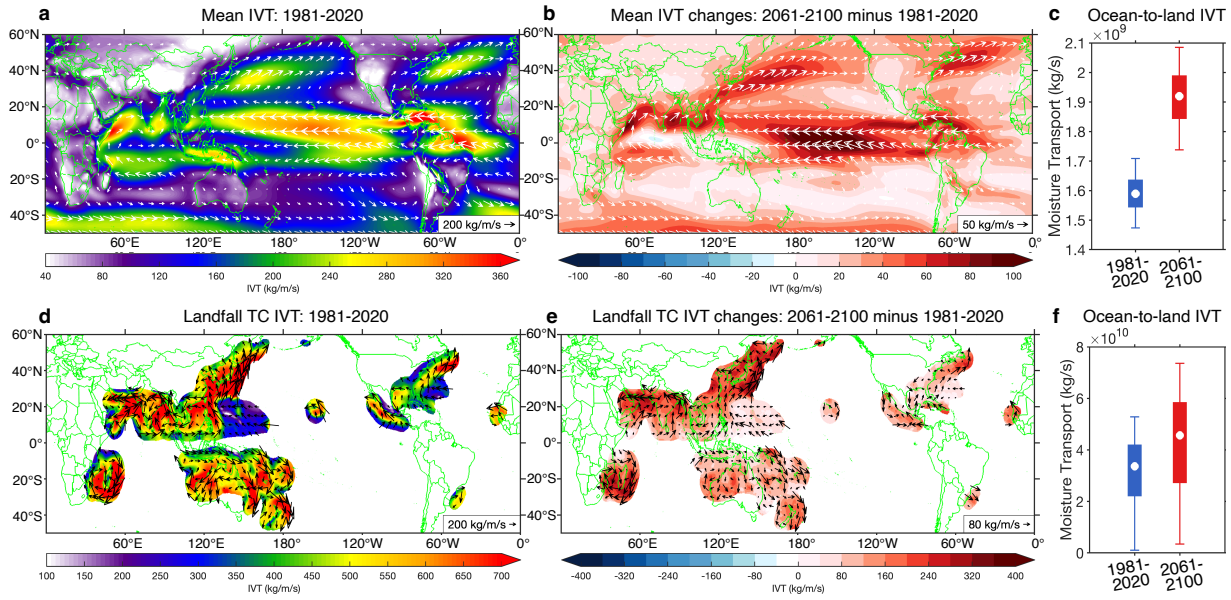

Supplementary Figure 7. Large-scale and TC associated integrated water vapor transport (IVT; unit: kg/m/s) in CESM-HR. 10-member ensemble averaged large-scale (**a**)1981-2020 historical mean IVT and (**b**) projected future changes between 2061–2100 and 1981–2020. (**c**) The box-whisker plots show the median (white dot), interquartile range (boxes), and 5th to 95th percentile (whiskers) of ocean-to-land total moisture transport (units: kg/s) during these two periods across 10-member ensemble. The large-scale mean ocean-to-land moisture transport increases by 0.3 × 10^9 kg/s (+18.8%), from 1.6 × 10^9 kg/s in 1981–2020 to 1.9 × 10^9 kg/s in 2061–2100. (**d-f**) Are similar to (**a-c**), but for landfalling TC-associated IVT. The TC-associated ocean-to-land moisture transport increases by 1.1 × 10^{10} kg/s (+35.5%), from 3.1 × 10^{10} kg/s in 1981–2020 to 4.2 × 10^{10} kg/s in 2061–2100.

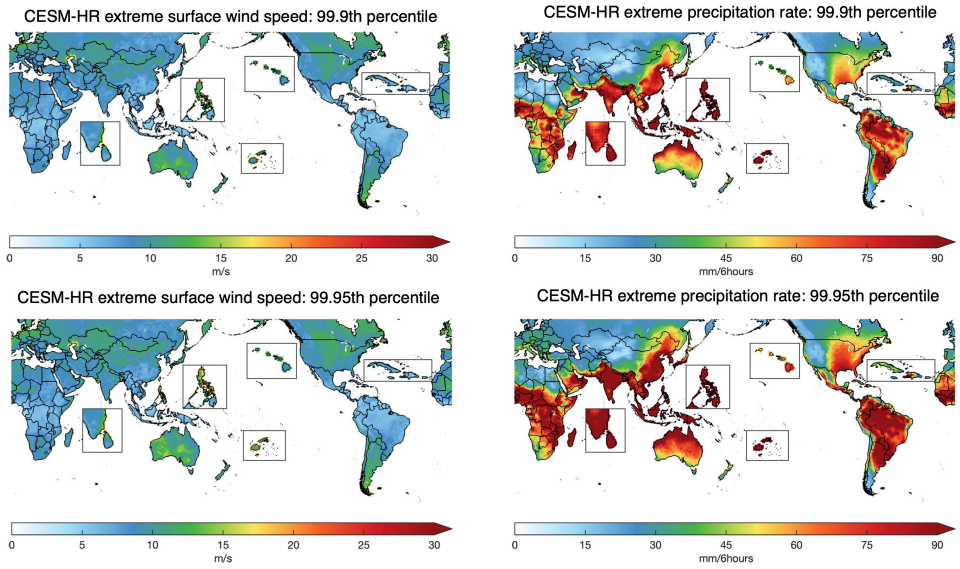

Supplementary Figure 8. Extreme surface wind (units: m/s; left column) and precipitation rate (units: mm/6 hours; right column) values in the 10-member CESM-HR ensemble for the 1981-2020 period. The 99.9th and 99.95th percentile extreme values are shown in the top and bottom panels, respectively. To compute these extreme values, we concatenated all 6-hourly data from the 10-member ensemble during 1981-2020 and derived the 99.9th and 99.95th percentile values. These extreme values are calculated regardless of TCs.

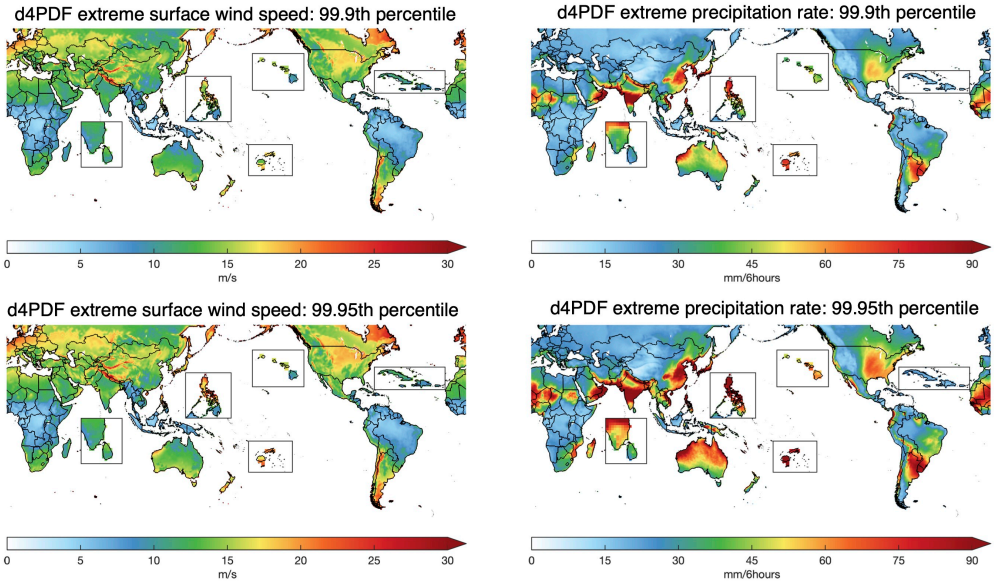

Supplementary Figure 9. Similar to Supplementary Figure 8, but for extreme surface wind (m/s) and precipitation rate (mm/6 hours) values in the 100-member d4PDF ensemble for the 1971-2010 period.